archives
of thermodynamics
Vol. **42**(2021), No. 1, 163–182
DOI: 10.24425/ather.2021.136953

Thermal efficiency and hydraulic performance evaluation on Ag–Al_2O_3 and SiC–Al_2O_3 hybrid nanofluid for circular jet impingement

ABANTI DATTA*
PABITRA HALDER

Indian Institute of Engineering Science and Technology, Shibpur PO: Botanic Garden, Howrah-711103, West Bengal, India

Abstract Hybrid nanofluids is obtained by dispersing more than one nanoparticle into a base fluid. The work is concerned with a detailed numerical investigation of the thermal efficiency and hydraulic performance of hybrid nanofluids for circular jet impinges on a round plate. For this paper, a metal (Ag), a metal oxides (Al_2O_3) and a metal carbides (SiC) nanoparticle and their water based hybrid nanofluids are considered to analyse numerically with varying significant dimensionless parameters, i.e., the jet-to-plate spacing ratio, Reynolds number and volume fraction of nanoparticles. The results demonstrated that the efficiency of heat transfer of all nanofluids is increased by the addition of nanoparticle to the dispersed in water at constant Reynolds number. Moreover, the results illustrate that heat transfer efficacy and pumping power penalty both increased as jet-to-plate spacing ratio reduced. The jet-to-plate spacing ratio equal to 4 is the best as the percentage enhance heat transfer is maximum in this situation. Since both the heat transfer effect and pumping penalty increase using hybrid nanofluids, thermal performance factor increases or decreases depends on nanoparticles of nanofluids. It is evident that the analysis of these hybrid nanofluids will consider both the increase in heat efficiency and the pumping capacity. The best flow behaviour is achieved for SiC–Al2O3 hybrid nanofluids. New merit number is introduced for additional clarification.

Keywords: hybrid nanofluid; thermal performance factor; pumping power; merit number

*Corresponding Author. Email: abanti.datta@gmail.com

Nomenclature

C_P	–	specific heat
D	–	diameter of jet
f	–	friction factor
H	–	enthalpy, distance between slot and heated plate
h	–	average convective heat transfer
k	–	turbulent kinetic energy
M	–	merit number
Nu	–	Nusselt number
n	–	number of phases
PP	–	pumping power
R	–	radius of the round plate
Re	–	Reynolds number
T	–	thermodynamic temperature
T_J	–	inlet temperature of jet
T_H	–	temperature of heated plate
TPF	–	thermal performance factor
U	–	inlet velocity of jet
$\vec{V}_m$	–	mass-averaged velocity
$\vec{V}_{dr}$	–	drift velocity

Greek symbols

η	–	Einstein coefficient
λ	–	thermal conductivity
μ	–	dynamic viscosity
ρ	–	density
σ	–	Prandtl number
ϕ	–	concentration of nanoparticles
ω	–	specific dissipation rate of k

Subscripts and superscripts

bf	–	base fluid
hnf	–	hybrid nanofluid
m	–	mixture
nf	–	nanofluid
p	–	primary phase
$p1$	–	Al_2O nanoparticle
$p2$	–	Ag and SiC nanoparticles
s	–	secondary phase
T	–	transpose vector

1 Introduction

Nanofluids jet impingement simulation has a significant role for cooling applications. The most critical problem concerning the cooling of electronic data processing, whether an electronic chip can dissipate heat rapidly and efficiently, became the focus of investigate on heat exchange equipment. The jet directs perpendicularly to the destination surface and allows high heat transfer in the region of impinging. The implementation of jet is sort of high-heat transfer coefficient dissipation process that is commonly used in many fields. The jet impinging flow gives a greater turbulence and improved heat exchange and mass exchange efficiency compared to the other laminar flow. Their coefficient of heat transfers several times of magnitude above the traditional convective coefficient of heat transfer [1].

A new type of thermal transmission fluids are hybrid nanofluids. This is also a process used to combine various material properties to resolve a variety of inconveniences in a single material. Several experimental studies and theoretical analysis have confirmed the convenient performance of nanofluids over the past two decades. Now, the heat and mass transfers research community's attention grow to hybrid nanofluids due to nanoparticles contain large surface energy with a specific surface region. Hybrid nanofluids are dispersed in one fluid and that combine the advantages of improved thermal conductivity of both mono and composite fluid to maintain the viscosity at lower values [1–10]. Despite the lack of clarification on basic nanofluid behaviour, research findings on hybrid nanofluids are promising. Nanoparticles formed and suspended in water were nevertheless thought to be a better method of most researchers (see, for example, works conducted by Madhesh and Kalaiselvam [11], Suresh *et al.* [12], Jana *et al.* [13], Abbasi *et al.* [14], and Nine *et al.* [15]). It is significant that most research have recognized that thermal conductivity is increasing [16] and that the heat transfer efficiency is increasing [17–19].

Many studies have presented the thermal conductivity to a certain degree to the configuration of new microstructures of various nanoparticles [20–26]. Sarkar *et al.* [27] outlined in recent years the thermophysical properties, pressure drop and heat exchange properties of mixed nanofluid and determined that proper hybridization of nanofluid would improve hybrid transmission efficiency because of the synergistic effect and strong aspect ratio of nano materials. Moghadassi *et al.* [28] have examined nanofluid effects on heat exchange in laminar flow using fluid dynamics model. They showed that hybrid nanofluids have a high convection heat transfer coefficient. Moreover, as related with Al_2O_3–water the average Nusselt number of Al_2O_3–Cu–water hybrid nanofluid has risen by 13.46% and 4.73%, respectively. Esfe *et al.* [29] have studied artificial neuronal systems for the study of thermal conductivity of the hybrid nanofluid SWCNT–MgO–EG (single walled carbon nanotube-magnesium oxide-ethylene glycol). The study showed that hybrid nanofluid thermal conductivity was substantially higher for SWCNT–EG nanofluid than that of MgO–EG nanofluids. With the increment of volume concentration of nanoparticle, the thermal conductivity increased.

Al_2O_3–Cu powders were considered by ray diffraction and scanning of the electron microscopic in Suresh *et al.* [30]. Their experimental findings revealed that, in contrast with water, the average Nusselt number of Al_2O_3–Cu–water hybrid nanofluids increased by 10.94%. Esfe *et al.* [31] have examined thermal conductivity of 0.02–1.0% solid-volume ZnO–multiwall carbon nanoparticles–ethylene glycol–water hybrid nanofluid. Experiments have shown that thermal conductivity is rising linearly at low concentrations. The effect of the temperature on hybrid nanofluid's thermal conductivity was highly nonlinear at high concentrations.

In order to build nanofluid in one step process, the Munkhbayar *et al.* [32] have dispersed silver nanoparticle into multiwall carbon nanoparticles/water. The microscopic scan-electron revealed the uniform distribution of silver nanoparticles around the multiwall carbon nanotube wall. The observation demonstrated an improved distribution and thermal conductivity of nanofluids by addition of silver nanoparticles, and an improvement in thermal conductivity of 14.5%. Minea [33] informed about heat transfer enhancement and pumping power on tube using hybrid nanofluid. She studied numerically on metal oxides nanofluid and their hybrid. She proposed a new coefficient to estimate of nanofluids behaviour.

On the basis of the insights garnered from existing research it can be said that further studies are still required where the beneficial effect of water substitution is verified for jet impingement by water-based nanofluids. As per authors knowledge, thermal performance factor and pumping power effect scarcely reported using hybrid nanofluid on circular jet impingement. Therefore, a detailed numerical analysis on turbulent jet impingement flow was conducted in this paper, outlining impact on the heat transfer efficiency and pumping power of different types of nanoparticle and volume concentrations. This research is supposed to be useful, as most investigators speak about the benefits of nanofluids while the discussion of pumping power drawbacks is significant for jet impingement cooling application of fluid mechanics. New merit number is introduced for evaluation of hybrid nanofluids performance in complicated systems such as electronics cooling.

2 Mathematical modelling

2.1 Geometrical configuration and boundary condition

Figure 1 shows an axisymmetric flow domain which illustrate a circular jet impinges on hot isothermal round plate using nanofluid, is investigated numerically for evaluating thermal and fluid dynamic performance. Circular jet diameter is donated as D and round plate radius is donated as R. Jet to plate spacing is H. The jet is impinged in the flow domain with a jet velocity U and temperature, $T_J = 298$ K. The top surface of the domain is assumed to adiabatic wall whereas isothermal with temperature $T_H = 348$ K is applied on bottom surface. Right side of boundary is considered as pressure outlet boundary while left side boundary is symmetric.

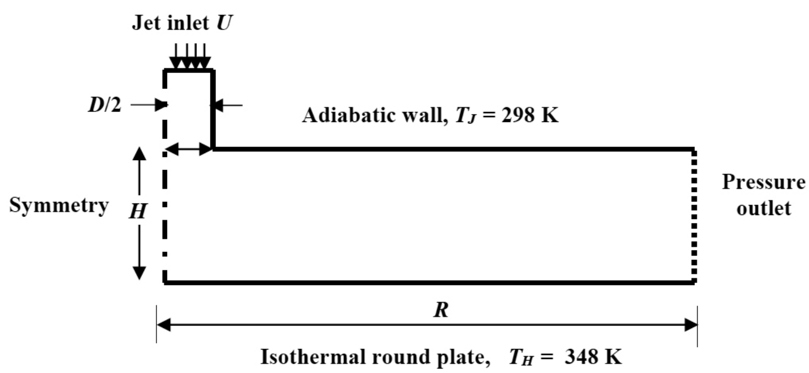

Figure 1: Schematic diagram of impinging jet with boundary conditions.

2.2 Governing equations and turbulence modelling equations

The analysis is carried out assuming the mixture to be a two-phase fluid with improved the properties due to the addition of nanoparticles with varying concentrations. Both phases are believed to be moving at the same speed. Continuity, energy and momentum equations for the mixture are resolved in a mixture model approach while for secondary phase volume concentration equation is calculated. The volume fraction of the particles is further determined from each discrete phase's continuity equation

$$\nabla \cdot \left(\rho_m \vec{V}_m\right) = 0\,, \tag{1}$$

where $\vec{V}_m$ is mass-averaged velocity and ρ_m the is mixture density.

Momentum equation

$$\varphi \nabla \cdot \left(\rho_m \vec{V}_m \vec{V}_m\right) = -\nabla p + \nabla \cdot \left[\mu_m \left(\nabla \vec{V}_m + \nabla \vec{V}_m^T\right)\right] + \rho_m \vec{g} + \nabla \cdot \left(\sum\nolimits_{s=1}^{n} {}_s\rho_s \vec{V}_{dr,s} \vec{V}_{dr,s}\right), \tag{2}$$

where p is the pressure, μ_m is the mixture viscosity, $\vec{V}_{dr,s}$ is the secondary phase drift velocity, ρ_s is the secondary phase density and φ_s is the secondary phase volume fraction, $\vec{g}$ is the gravitational acceleration, and n is the number of phases.

Energy equation

$$\lambda \nabla \cdot \left[\sum_{s=1}^{n} \phi_s \vec{V}_s \left(\rho_s H_s + p\right)\right] = \nabla \cdot \left({}_m \nabla T - C_{P,m} \rho_m \overline{vt}\right), \tag{3}$$

$$\nabla \left(\phi_p \rho_p \vec{V}_m\right) = -\nabla \left(\lambda \nabla T - \phi_p \rho_p \vec{V}_{dr,p}\right), \tag{4}$$

where H_S is the enthalpy of the secondary phase, T is the thermodynamic temperature, λ and λ_m are the effective thermal conductivity and thermal conductivity of the mixture, respectively, $\vec{V}_{dr,p}$ is the primary phase drift velocity, ϕ_p is the primary phase volume fraction, ρ_p primary phase density, C_P is the specific heat, $C_P \rho_m \overline{vt}$ is turbulent heat flux and $\overline{vt}$ is turbulent viscosity.

Compression and viscous dissipation in the conservation of energy Eq. (4) are considered to be marginal. The relative speed is determinate by the expressions defined by Manninen *et al.* [34] for the conservative momentum Eq. (2), whereas the drag function is computed by the related expressions provided by Schiller and Naumann [35]. Experimental or approximate models in the turbulent flows would take the turbulence phenomenon into account for the implementation of governing equations. It has been suggested that k-ω SST (shear stress transport) turbulence model should be applied to confined jet impingement according to Sagot *et al.* [36] and Menter [37]. The k-ω SST models of turbulence have two equations:

$$\nabla \cdot \left(\rho_m \vec{V}_m k\right) = \nabla \left[\left(\mu + \frac{\mu_t}{\sigma_k}\right) \nabla k\right] + G_k - Y_k\,, \tag{5}$$

$$\nabla \cdot \left(\rho_m \vec{V}_m \omega\right) = \nabla \left[\left(\mu + \frac{\mu_t}{\sigma_\omega}\right) \nabla k\right] + G_\omega - Y_\omega + D_\omega \,, \tag{6}$$

where k is the turbulent kinetic energy, ω is the specific dissipation rate of k, μ, and μ_t are the dynamic viscodity and turbulent eddy viscosity respectively, G_k stands for turbulent kinetic energy output, mean speed gradients, and G_ω stands for generating the specific dissipation rate of ω, Y_k and Y_ω are the dissipation of k and ω to turbulence, D_ω is a cross-diffusion term, σ_k and σ_ω are turbulent Schmid and turbulent Prandtl number, respectively, for k and ω.

2.3 Thermophysical properties of hybrid nanofluid

In this paper, the hybrid nanofluid is a mixture of $Ag+Al_2O_3$ and $SiC+Al_2O_3$ nanoparticles and water (base fluid). The fraction of nanoparticles is applied as 1%, 1.5%, and 2%. The physical properties of all nanoparticles are given in Table 1.

Table 1: Thermophysical properties of nanoparticles and water.

Material	Density (kg/m^3)	Specific heat (J/kg K)	Dynamic viscosity (Pa s)	Thermal conductivity (W/m K)
Water	998.2	4182	998×10^{-6}	0.597
Al2O3	3880.0	773	–	36.0
Ag	10500	235	–	429
SiC	3160	1340	–	350

The effective density of the hybrid nanofluid, similar to single nanofluid, can be defined by its mass balance. The density of hybrid nanofluid is calculated as

$$\rho_{hnf} = \phi_{p1}\rho_{p1} + \phi_{p2}\rho_{p2} + (1-\phi)\rho_{bf} \,, \tag{7}$$

$$\phi = \phi_{p1} + \phi_{p2} \,. \tag{8}$$

Here ρ_{bf} is the density of base fluid (water and) ϕ is the overall fraction of two separate nanoparticle dispersed in hybrid nanofluid, $p1$ is denoted for Al_2O_3 nanoparticle and $p2$ is for Ag and SiC nanoparticles.

The specific heat of the hybrid nanofluid is calculated as follows, by applying energy balance similar to single nanofluid:

$$C_{Phnf} = \phi_{p1}\rho_{p1}C_{Pp1} + \phi_{p2}\rho_{p2}C_{Pp2} + (1-\phi)\, C_{Ppbf}\rho_{hnf} \,. \tag{9}$$

The Krieger–Dougherty relation is shown to be an efficient pattern for relating the viscosity of non-accumulating colloidal dispersions or nanofluids to the particle volume concentration for higher volume concentration [38]:

$$\mu_{hnf} = \left(1 - \frac{\phi}{\phi_m}\right)^{-\eta\phi_m} \tag{10}$$

where η is 2.5, and $\phi_m = 0.65$.

Many authors used the Maxwell model to estimate mono nanofluid heat conductivity [39]. By inserting an average thermal conductivity solid nanoparticle, the thermal conductivity of the hybrid nanofluid can be evaluated and the updated Maxwell model can therefore be written by

$$k_{hnf} = k_{bf}\left[\frac{\dfrac{\phi_{p1}k_{p1} + \phi_{p2}k_{p2}}{\phi} + 2k_{bf} + 2\left(\phi_{p1}k_{p1} + \phi_{p2}k_{p2}\right) - 2k_{bf}}{\dfrac{\phi_{p1}k_{p1} + \phi_{p2}k_{p2}}{\phi} + 2\phi k_{bf} - \left(\phi_{p1}k_{p1} + \phi_{p2}k_{p2}\right) - \phi k_{bf}}\right]. \tag{11}$$

3 Results and discussion

The average heat transfer and pumping power characteristics of hybrid nanofluid circular jet impinges on round plate have been assessed. As the water is a conventional coolant for the electronics cooling, the water has been taken as the base fluid. The analysis is simulated on hybrid nanofluids Ag–Al_2O_3 and SiC–Al_2O_3 by using metal (Ag), metal oxides (Al_2O_3) and metal carbides (SiC) nanoparticle. The thermophysical properties of Ag, SiC, and Al_2O_3 nanoparticle are calculated from Table 1. Finite volume method is applied to resolve the boundary conditions with coupled nonlinear differential equations. The pressure-based commercial solver (Ansys Fluent) [40] is applied for the numerical computations. The energy and momentum equations are resolved by 2nd order upwind interpolation scheme, while the normalized residual reduces lesser than 10^{-9} for the energy equation and under 10^{-6} for all other variables, the solution is assumed to converge. The jet is entered in the flow field with a velocity U and temperature $T_J = 298$ K. On left side of the domain symmetry boundary condition and on right side of the domain pressure outlet condition are applied. The impingement round plate is kept at a temperature $T_H = 348$ K.

To obtain results concerning the heat transfer enhancement and pumping power, the total nanoparticle concentration has been varied as 1%, 1.5%, and 2%. The study also done on varying the inlet jet velocity based on

Reynolds number (Re $= 10\,000$, $20\,000$, and $30\,000$) and changing the jet to plate ratio ($H/D = 2$, 4, and 6). Doing this has led to obtaining results for changing geometry and nanofluid properties, as well as changing heat transfer improvement and pumping power.

3.1 Grid sensitivity and validation

A grid implementation of $y^+ = 1$ (nondimentionalized wall normal distance) for k-ω SST model on a viscous sublayer is presented with the nonuniform grid. Four distinct grid distributions are performed on Reynolds number Re $= 30\,000$ and $H/D = 6$ for grid independent analysis. The distributions in the grid are conducted on 300×100, 280×90, 260×80, and 240×70 (number of grid nodes). As the Nusselt number distribution has no significant change for grid 300×100, the rest of the simulations done on grid 300×100.

Before working on actual problem, an organized code justification and performance assessment of the SST k-ω turbulence models are conducted. For that, simulation has been carried out with uniform inlet jet velocity corresponding to Reynolds number equal to $10\,000$ and H/D ratio of the flow field is equal to 2. Figure 2 showed that the comparison between the Nusselt

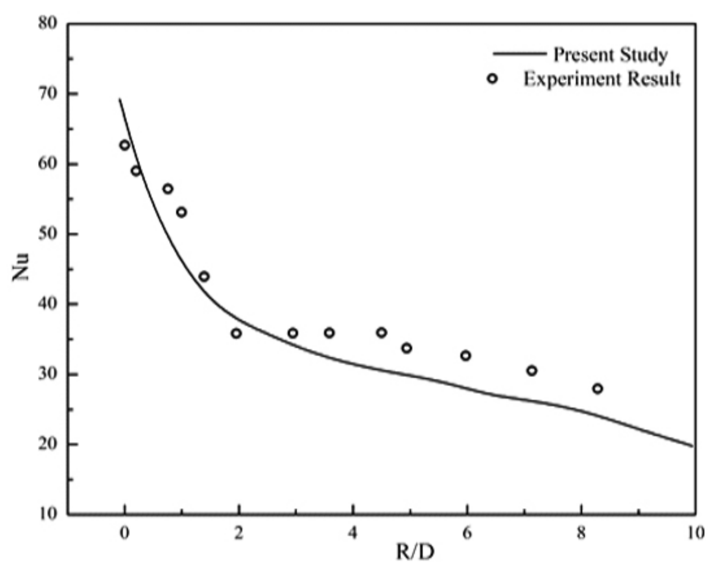

Figure 2: Present model is validated with experimental data from Sagot [36].

number profile and experimental Nusselt number profile of Sagot [36]. The experimental settings consist of 2.4 mm diameter of jet and 2.4 mm radius of round plate [36]. The value of local Nusselt number in impingement plate is little high at at low R/D ratio then it decreases with increasing R/D ratio. There was strong agreement with the experimental outcome on the Nusselt number distribution profile.

3.2 Average convective heat transfer coefficient

It should be noted that the heat transfer coefficient is selected over the Nusselt number to compare the effectiveness of the thermal transfer. It is because the Nusselt number underestimates the thermal conductivity increasement of the nanofluids. The average convective heat transfer ratio can be stated by the following equation [41]:

$$h = \frac{h_{nf}}{h_{bf}}, \quad (12)$$

where h is the average convective heat transfer ratio and h_{nf} and h_{bf} are the average convective heat transfer of nanofluid and base fluid, respectively.

In Fig. 3 percentage of the average convective heat transfer coefficient enhancement for considered nanofluids (mono and composite component) compared with water is shown. Figure demonstrated numerical results considering the overall volume concentration of nanoparticles dispersed in the

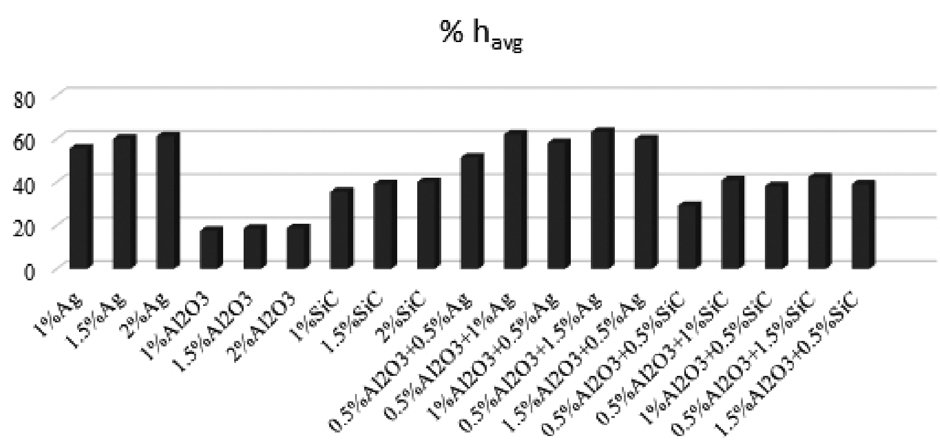

Figure 3: Average convective heat transfer coefficient enhancement percentage at $H/D = 4$ and $\mathrm{Re} = 10\,000$.

water. The highest percentage of heat transfer for Ag-water-based nanofluid is obtained, while the Al_2O_3–water nanofluid has the lowest percentage. However, both hybrids have a good thermal behaviour: for Al_2O_3–Ag hybrid nanofluid, the heat transfer coefficient is 61% at 2% in volume (precisely 1.5% Ag+0.5% Al_2O_3). Therefore, it explained the improvement of the heat transfer resulting from the loading of nanoparticles and increased nanoparticles are transmitted mainly by higher thermal conductivity. In Al_2O_3–Ag hybrid nanofluid it is observed to have a higher concentration Ag (1.5% Ag + 0.5% Al_2O_3) in contrast to a higher concentration of Al_2O_3 (0.5% Ag +1.5% Al_2O_3) in the same overall volume. The result is a significant increase of heat transfer in former.

It is exciting to note that previously discussed adverse effects due to H/D ratio increased irrespective to the Reynolds number. When the H/D value increased from 2 to 6, the heat efficacy of nanofluid first increased and then continued to decline with the same Reynolds number. At $H/D = 4$, the heat efficacy reached its highest value as shown in Fig. 4. For a constant value of Reynolds number, the coefficient of heat transfer decreases significantly with an increased H/D ratio (Fig. 5). Furthermore, with different Reynolds number for the same single or hybrid nanofluid, heat transfer coefficient remains nearly constant.

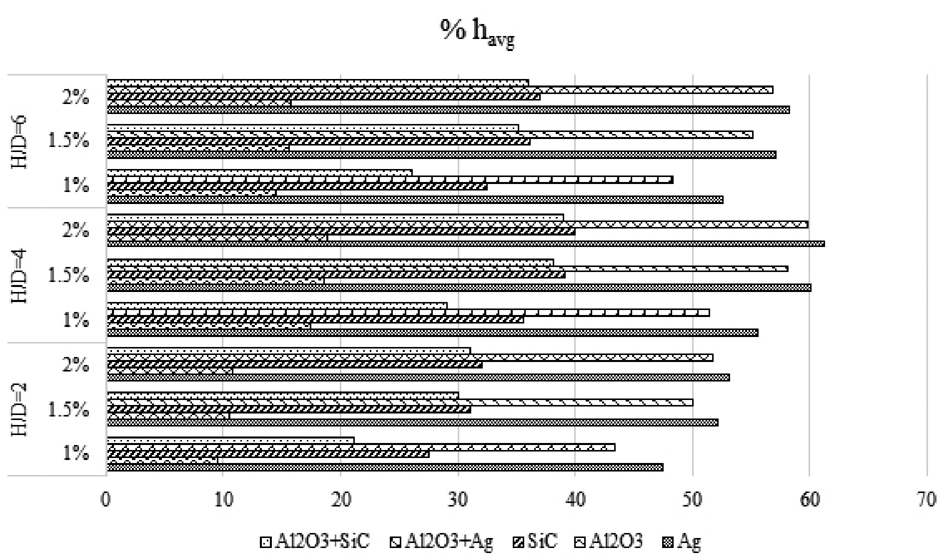

Figure 4: Average convective heat transfer coefficient enhancement percentage at Re = 10 000 and $H/D = 2$, 4, and 6.

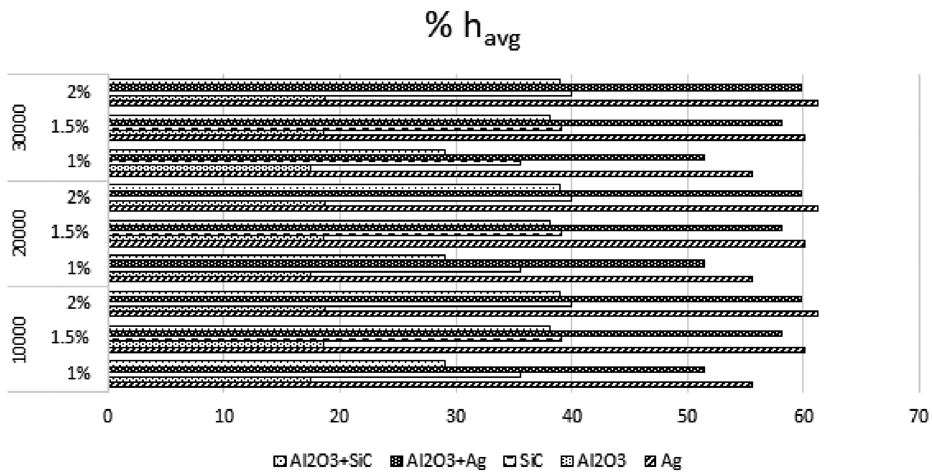

Figure 5: Average convective heat transfer coefficient enhancement percentage at $H/D = 4$ and Re = 10 000, 20 000, and 30 000.

3.3 Pumping power

The goal of this research is to obtain a numerical outline for pumping power for hybrid nanofluids using metal (Ag), metal oxides (Al_2O_3) and metal carbides (SiC), as stated in the introduction. Similar to the average heat transfer coefficient, it is easier to report the effects of the relative pump power or pumping ratio (PP), which is more common than the pumping power. The relative pump power is measured as the ratio of the nanofluid pumping power to the water pumping power. With a value greater than 1, the nanofluid requires to boost pumping power compared to the base fluid and thus need to pump an additional energy for jet impingement, which will affect overall energy efficacy. The pumping power ratio can be stated by the following equation [41]:

$$\mathrm{PP} = \frac{\mathrm{PP}_{nf}}{\mathrm{PP}_{bf}}, \tag{13}$$

where PP_{nf} and PP_{bf} are the pumping power of nanofluid and base fluid, respectively.

Figure 6 portrays the numerical result for the pumping power of all hybrid nanofluid and mono nanofluid. The pumping power ratio is calculated from the simulated pressure drop. The addition of nanoparticles to a basis fluid, as predicted, will not only improve heat transfer but also rise pressure losses or stress in the wall shear. Pumping power increases as nanoparticles are suspended, in most instances can easily be seen. The increase of pumping power for Ag–Al_2O_3 hybrid nanofluid is nearly 7.3 times and Al_2O_3 nanofluid also has high pumping penalty. Some instances of SiC–Al_2O_3 hybrid (*i.e.* high concentration of SiC) and SiC nanofluid have less pumping power penalty. With regard to the increased pumping power induced by loading the nanoparticles, it is evident that higher pumping power is due mainly to increased pressure drops (Fig. 6). In Fig. 7, the Pumping power increases with the decreased H/D ratio for a constant value of Reynolds number. Moreover, with different Reynolds number for the same nanofluids (single or hybrid), the pumping power increased as shown in Fig. 8.

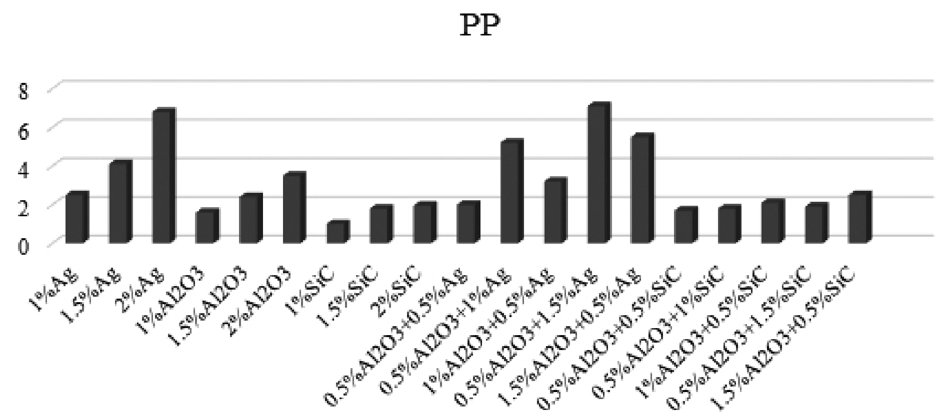

Figure 6: Pumping power at $H/D = 4$ and $\mathrm{Re} = 10\,000$.

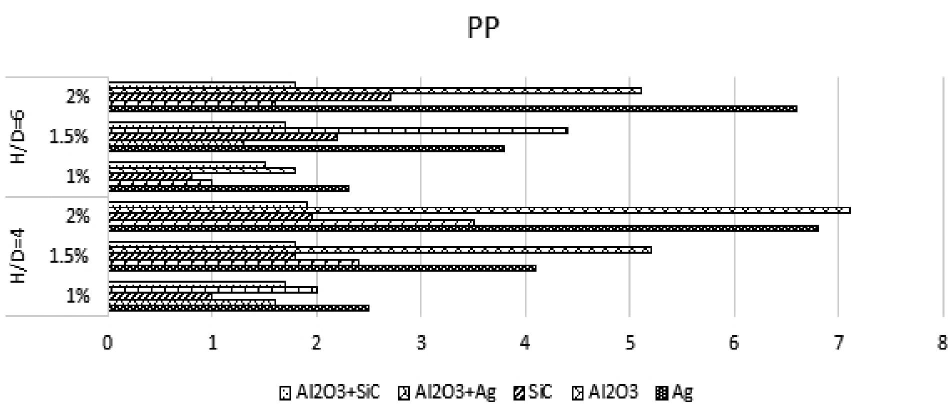

Figure 7: Pumping power at $H/D = 4$ and $\mathrm{Re} = 10\,000$.

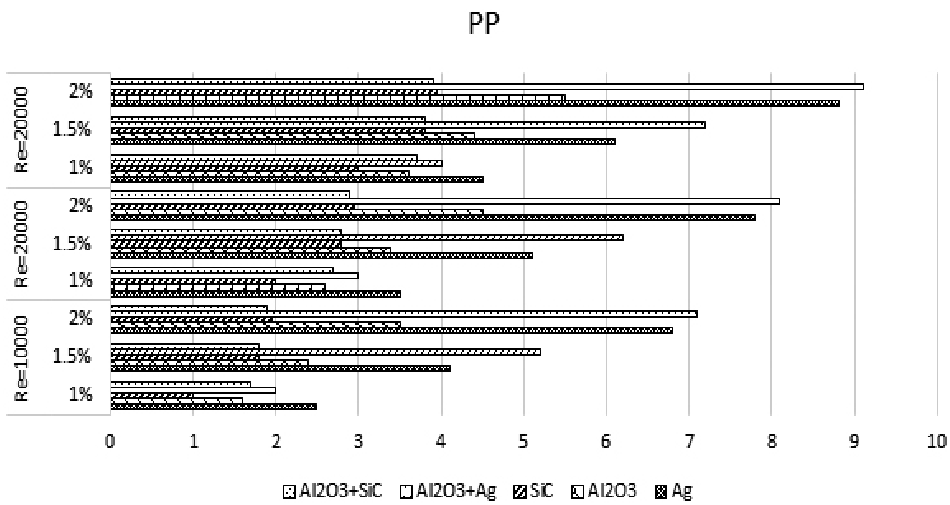

Figure 8: Pumping power at $H/D = 4$ and Re= 10 000, 20 000, and 30 000.

3.4 Thermal performance factor

The energetic or thermal efficiency of fluid in a particular system can be defined in several ways. Author have considered the thermal performance factor (TPF), which increases or decreases depends on nanoparticles of nanofluid as both the heat efficacy and pumping penalty rise using hybrid nanofluids. Hence, the thermal performance factor is significant parameter to the design heat transfer application. The TPF can be determined by the following equation [42]:

$$\mathrm{TRF} = \frac{\dfrac{\mathrm{Nu}_{hnf}}{\mathrm{Nu}_{bf}}}{\left(\dfrac{f_{hnf}}{f_{bf}}\right)^{1/3}}, \tag{14}$$

where Nu_{bf} is the base fluid Nusselt number and f_{bf} is friction factor. Nu_{hnf} and f_{hnf} are the hybrid nanofluid Nu number and friction factor, respectively. If TPF is below 1.0 the thermal power is below the hydraulic efficiency. Therefore, nanofluid or hybrid nanofluid is not advantageous in terms of heat transfer. If TPF exceeds 1.0 thermal efficiency exceeds hydraulic output. Thus, nanofluid or hybrid nanofluid is feasible for surface cooling.

Figure 9 shows that TPF declines by 2.8 times in Ag–Al_2O_3 hybrid nanofluid and SiC–Al_2O_3 hybrid nanofluid has higher thermal performance factor. The TPF results presents that each individual nanofluid perform very well both in Nusselt number and in friction factor, while TPF is larger than 1 for the most hybrid nanofluids. The reasons are complex, including the combination of improved thermal conductivity and an increase of nanofluid viscosity. In the boundary layer the thermal diffusion resistance of laminar sublayer decreases as thermal conductivity improved. Though, resistance to heat transmission increased while viscosity surges the sublayer's thickness. Hence, the conclusions from Figs. 3 and 6 are discussed further. The result of average heat transfer increase from 1% to 62%, depending on the category of nanoparticles and the volume concentrations. From Fig. 3 it is evident that all mono nanofluid and hybrid nanofluid perform better than base fluid, *i.e.* water. Though pumping power increases with the concentration of nanoparticles, for SiC–Al_2O_3 hybrid nanofluids the least increases are recorded (Fig. 6).

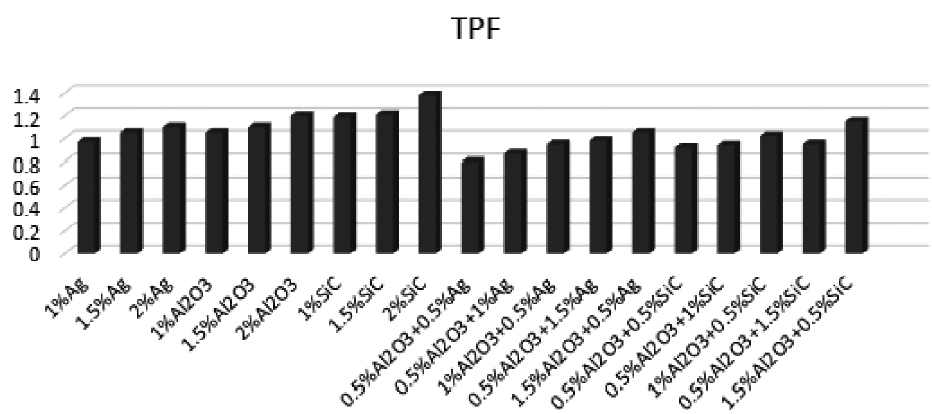

Figure 9: TPF comparison for hybrid and single nanofluids.

3.5 Nanofluid merit parameter

For further clarification author have studied another parameter to investigate maximum output regarding thermal and hydraulic evaluation. In enhanced circumstances of heat transfer the idea of the penalty of pumping power is also used as a measure of comparison and in some applications, it is more sensible. In this analysis, the heat transfer is combined with pumping power to produce a parameter that indicates overall merit of hybrid as well as single nanofluid, is calculated based on constant flow velocity.

Merit number is the ratio of enhanced heat transfer to pumping power increment:

$$\mathrm{M} = \frac{\dfrac{h_{hnf}}{h_{bf}}}{\dfrac{\mathrm{PP}_{hnf}}{\mathrm{PP}_{bf}}} \tag{15}$$

where h_{hnf} is the heat transfer coefficient of hybrid nanofluid and h_{bf} is heat transfer coefficient of base fluid, and PP_{hnf} and PP_{bf} are the pumping power of hybrid nanofluid and base fluid, respectively.

A higher merit value means that there is a greater improvement in heat transfer than the pumping power penalty. Consequently, lower merit value is while pumping power larger than heat duty. The net effect of these competing phenomena depends on the magnitude of merit number as illustrated in Fig. 10. After correlating the all data, it may be confirmed the best flow behaviour is achieved by SiC–Al_2O_3 hybrid nanofluids in replacement of water. Since it is evident that SiC–Al_2O_3 hybrid nanofluids have higher heat enhancement compare to its pumping penalty. Precisely, 42.2% increase in average heat transfer coefficient and 17% increase pumping power is achieved for 1.5% SiC + 0.5% Al_2O_3 hybrid nanofluid.

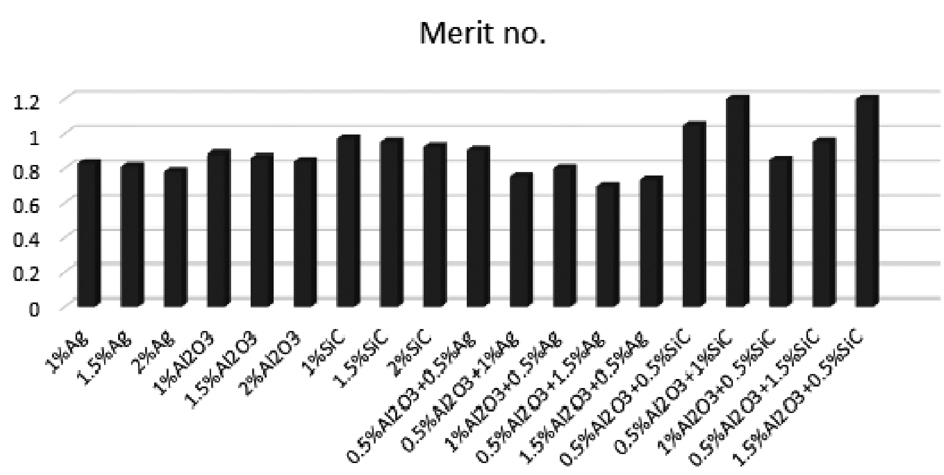

Figure 10: Merit number comparison for hybrid and single nanofluids.

4 Conclusions

The present paper numerically investigated of three type of single nanofluids (Al_2O_3, SiC, and Ag suspended in water) and two hybrid nanofluids (SiC–Al_2O_3 and Ag–Al_2O_3). The numerical analysis is performed on round plate which is impinged by circular jet with varying significant dimensionless parameter such as H/D ratio (2, 4, and 6), Reynolds number (10 000, 20 000, and 30 000) and volume concentration of nanoparticles (1%, 1.5%, and 2%). Thermal and hydraulic performance assessment are discussed.

Heat transfer capacity of all nanofluids is enhanced by adding nanoparticles which is suspended on water at the constant Reynolds number. If the jet to plate ration H/D raised from 2 to 6, the heat efficacy first increased and then declined with the same Reynolds numbers. At $H/D = 4$, the value of thermal efficiency is higher. As the pressure drop changes according to type and volume concentration of nanoparticle pumping power will increase as the concentration of nanoparticles increases. It can be noted that both the increasing heat transfer and pumping capacity is taken into account for these hybrid nanofluids. After correlating the heat duty and pumping penalty the best flow is achieved by Al_2O_3–SiC hybrid nanofluids. It can be concluded that an increase of 42.2% in the convective average heat transfer coefficient, with 17% improvement in pumping power is accomplished by $Al_2O_3 + 1.5\%$ SiC of 0.5%. For further clarification on investigate maximum output regarding thermal and hydraulic evaluation merit number is introduced to calculated heat transfer as well as pumping power efficiency. This proposed merit number is useful for complicated systems such as electronics cooling, hot rolling technology to assess nanofluids performance.

Received 6 June 2020

References

[1] Sun B., Zhang Y., Yang D., Li H.: *Experimental study on heat transfer characteristics of hybrid nanofluid impinging jets.* Appl. Therm. Eng. **151**(2019), 556–566

[2] Vafaei M., Afrand M., Sina N., Kalbasi R., Sourani F., Teimouri H.: *Evaluation of thermal conductivity of MgO-MWCNTs/EG hybrid nanofluids based on experimental data by selecting optimal artificial neural networks.* Physica E (Low-dim. Sys. Nanostruct.) **85**(2017), 90–96.

[3] Kumar D.D., Arasu A.V.: *A comprehensive review of preparation, characterization, properties and stability of hybrid nanofluids.* Renew. Sustain. Energy Rev. **81**(2017), 2, 1669–1689.

[4] MINEA A.A.: *Challenges in hybrid nanofluids behavior in turbulent flow: recent research and numerical comparison*. Renew Sustain. Energy Rev. **71**(2016), 426–434.

[5] SIDIK N.A.C., ADAMU I.M., JAMIL M.M., KEFAYATI G.H.R., MAMAT R., NAJAFI G.: *Recent progress on hybrid nanofluids in heat transfer applications: a comprehensive review*. Int. Commun. Heat Mass **78**(2016), 68–79.

[6] NABIL M.F., AZMI W.H., HAMID K.A., ZAWAWI N.N.M., PRIYANDOKO G., MAMAT R.: *Thermo-physical properties of hybrid nanofluids and hybrid nanolubricants: a comprehensive review on performance*. Int. Commun. Heat Mass **83**(2017), 30–39.

[7] HAMZAH M.H., SIDIK N.A.C, KEN T.L., MAMAT R., NAJAFI G.: *Factors affecting the performance of hybrid nanofluids: a comprehensive review*. Int. J. Heat Mass Tran. **115**(2017), 12, 630–46.

[8] KHODADADI H., AGHAKHANI S., MAJD H., KALBASI R., WONGWISES S., AFRAND M.: *A comprehensive review on rheological behavior of mono and hybrid nanofluids: effective parameters and predictive correlations*. Int. J. Heat Mass Tran. **127**(2018), B, 997–1012.

[9] KUMAR D.D., ARASU A.V.: *A comprehensive review of preparation, characterization, properties and stability of hybrid nanofluids*. Renew. Sust. Energ. Rev. **81**(2018), 1669–89.

[10] SIDIK N.A.C., JAMIL M.M., JAPAR W.M., ADAMU I.M.: *A review on preparation methods, stability and applications of hybrid nanofluids*. Renew. Sust. Energ. Rev. **80** (2017), 1112–1122.

[11] MADHESH D., KALAISELVAM S.: *Experimental analysis of hybrid nanofluid as a coolant*. Procedia Eng. **97**(2014), 1667–1675.

[12] SURESH S., VENKITARAJ K.P, SELVAKUMAR P., CHANDRASEKAR M.: *Synthesis of* Al_2O_3*—Cu/water hybrid nanofluids using two step method and its thermophysical properties*. Colloids Surface A Physicochem. Eng. Asp. **388**(2011), 41–48.

[13] JANA S., KHOJIN A.S.,.ZHONG W.H: *Enhancement of fluid thermal conductivity by the addition of single and hybrid nano-additives*. Thermochim. Acta **462**(2007), 1–2, 45–55.

[14] ABBASI S.M., NEMATI A., RASHIDI A., ARZANI K.: *The effect of functionalization method on the stability and the thermal conductivity of nanofluid hybrids of carbon nanotubes/gamma alumina*. Ceram. Int. **39**(2013), 3885–3891.

[15] NINE M.J., MUNKHBAYAR B., RAHMAN M.S., CHUNG H., JEONG H.: *Highly productive synthesis process of well dispersed* Cu_2O *and* Cu/Cu_2O *nanoparticles and its thermal characterization*. Mater. Chem. Phys. **141**(2013), 636–642.

[16] CHEN L.F., CHENG M., YANG D.J., YANG L.: *Enhanced thermal conductivity of nanofluid by synergistic effect of multi-walled carbon nanotubes and* Fe_2O_3 *nanoparticles*. Appl. Mech. Mater. **548–549**(2014), 118–123.

[17] SUNDAR L.S., SINGH M.K., SOUSA A.C.M.: *Enhanced heat transfer and friction factor of MWCNT–Fe3O4/water hybrid nanofluids*. Int. Commun. Heat Mass **52**(2014), 73–83.

[18] BABY T.T., RAMAPRABHU S.: *Surfactant free magnetic nanofluids based on core-shell type nanoparticle decorated multiwalled carbon nanotubes*. J Appl. Phys. **110**(2011), 064325–31.

[19] Esfe M.H., Abbasian A.A., Rezaie M., Yan W.M., Karimipour A.: *Experimental determination of thermal conductivity and dynamic viscosity of Ag–MgO/water hybrid nanofluid*. Int. Commun. Heat Mass **66**(2015), 189–195.

[20] Das P.K.: *A review based on the effect and mechanism of thermal conductivity of normal nanofluids and hybrid nanofluids*. J. Mol. Liq. **240**(2017), 420–446.

[21] Soltani S., Kasaeian A., Sarrafha H. et al.: *An experimental investigation of a hybrid photovoltaic/thermoelectric system with nanofluid application*. Sol. Energy **155**(2017) 1033–1043.

[22] Leong K.Y., Ahmad K.Z., Ong H.C., Ghazali M.J., Baharum A.: *Synthesis and thermal conductivity characteristic of hybrid nanofluids — A review*. Renew. Sust. Energ. Rev. **75**(2017), 868–878.

[23] Nimmagadda R., Venkatasubbaiah K.: *Conjugate heat transfer analysis of microchannel using novel hybrid nanofluids (Al2O3 + Ag/Water)*. Eur. J. Mech. B. Fluids **52** (2015), 19–27.

[24] Sajid M.U., Ali H.M.: *Thermal conductivity of hybrid nanofluids: a critical review*. Int. J. Heat Mass Tran. **26**(2018), 211–234.

[25] Allahyar H.R., Hormozi F., Zarenezhad B.: *Experimental investigation on the thermal performance of a coiled heat exchanger using a new hybrid nanofluid*. Exp. Therm. Fluid Sci. **76**(2016), 324–329.

[26] Olatomide G.F., Adebimpe A.A., Ayodeji O.S., David O.O., Johnson A.O., Francis I.I., Fatai A.B.: *Numerical investigation and sensitivity analysis of turbulent heat transfer and pressure drop ofAl2O3/H2O nanofluid in straight pipe using response surface methodology*. Arch. Thermodyn. **41**(2020), 1, 3–30

[27] Sarkar J., Ghosh P., Adil A.: A review on hybrid nanofluids: recent research, development and applications. Renew. Sust. Energ. Rev. **43**(2015), 164–177.

[28] Moghadassi A., Ghomi E., Parvizian F.: *A numerical study of water based Al_2O_3 and Al_2O_3–Cu hybrid nanofluid effect on forced convective heat transfer*. Int. J. Therm. Sci. **92**(2015), 50–57.

[29] Esfe M.H., Rostamian S.H., Alirezaie A.: *An applicable study on the thermal conductivity of SWCNT-MgO hybrid nanofluid and price-performance analysis for energy management*. Appl. Therm. Eng. **111**(2016), 1202–1210.

[30] Suresh S., Venkitaraj K.P., Selvakumar P. *et al.*: *Effect of Al_2O_3–Cu/water hybrid nanofluid in heat transfer*. Exp. Therm. Fluid Sci. **38**(2012), 54–60.

[31] Esfe M.H., Esfandeh S., Saedodin S. *et al.*: *Experimental evaluation, sensitivity analyzation and ANN modeling of thermal conductivity of ZnO-MWCNT/EG-water hybrid nanofluid for engineering applications*. Appl. Therm. Eng. **125**(2017), 673–685.

[32] Munkhbayar B., Tanshen M.R., Jeoun J. *et al.*: *Surfactant-free dispersion of silver nanoparticles into MWCNT-aqueous nanofluids prepared by one-step technique and their thermal characteristics*. Ceram. Int. **39**(2013), 6, 6415–6425.

[33] Minea A.A.: *Pumping power and heat transfer efficiency evaluation on Al_2O_3, TiO_2 and SiO_2 single and hybrid water-based nanofluids for energy application*. J. Therm. Anal. Calorim. **139**(2020), 2, 1171–1181.

[34] Manninen M., Veikko T., Sirpa K.: *On the mixture model for multiphase flow.* VTT, Espoo 1996, 3–67.

[35] Schiller L., Naumann Z.: *A Drag Coefficient Correlation.* Zeitschrift des Vereins Deutscher Ingenieure **77**(1935), 318–320.

[36] Sagot B., Antonini G., Christgen A., Buron F.: *Jet impingement heat transfer on a flat plate at a constant wall temperature.* Int. J. Therm. Sci. **47**(2008), 12, 1610–1619.

[37] Menter F.R.: *Two-equation eddy-viscosity turbulence models for engineering applications.* AIAA J. **32**(1994), 8, 1598–1605.

[38] Krieger I.M.,. Dougherty T.J.: *A mechanism for non-Newtonian flow in suspension of 528 rigid spheres.* J. Trans. Soc. Rheol. **3**(1956), 37–152

[39] Maxwell J.C.: *A Treastise on Electricity and Magnetism* (2nd Edn.). Oxford Univer. Press, Cambridge 1881.

[40] *ANSYS Inc. ANSYS Fluent 15.0 UDF Manual*, Canonsburg, PA: ANSYS Inc, 2013.

[41] Gherasim I., Roy G., Nguyen, C.T., Vo-Ngoc, D.: *Heat transfer enhancement and pumping power in confined radial flows using nanoparticle suspensions (nanofluids).* Int. J. Therm. Sci. **50**(2011), 3, 369–377.

[42] Maradiya C., Vadher J., Agarwal R.: *The heat transfer enhancement techniques and their Thermal Performance Factor.* Beni-Suef Uni. J. Basic Appl. Sci. **7**(2018), 1, 1–21.